Journal of Hydrology, 77 (1985) 31—56
Elsevier Science Publishers B.V., Amsterdam — Printed in The Netherlands

[4]

VARIOGRAM IDENTIFICATION BY THE MEAN-SQUARED INTERPOLATION ERROR METHOD WITH APPLICATION TO HYDROLOGIC FIELDS

T. LEBEL and G. BASTIN

Institut de Mécanique de Grenoble, Groupe d'Hydrologie, Saint Martin d'Hères (France)
Laboratoire d'Automatique, de Dynamique et d'Analyse des Systèmes, Université Catholique de Louvain, 1348 Louvain la Neuve (Belgium)

(Received February 23, 1984; revised and accepted May 21, 1984)

ABSTRACT

Lebel, T. and Bastin, G., 1985. Variogram identification by the mean-squared interpolation error method with application to hydrologic fields. J. Hydrol., 77: 31—56.

. A systematic presentation of the "mean squared interpolation error" (MSIE) method for variogram identification is given. The presentation involves a theoretical analysis of the MSIE method under the (realistic) assumption that the parametric variogram model is only an approximation of the true-field variogram.

The application of the MSIE method to the identification of variogram models for a piezometric field and a rainfall field is described in some detail.

1. INTRODUCTION

Real-life applications of BLU (best linear unbiased) interpolation in random fields, require, in most cases, a preliminary identification of a parametric model for the variogram of the field of interest.

This identification is most often performed by a least-squares fitting (or even an intuitive fitting) of the parametric model to an "experimental" variogram. Numerous examples can be found in the books by David (1977), and Journel and Huijbregts (1978), and also, for hydrologic applications, in the papers by Delfiner and Delhomme (1975), Creutin and Obled (1982), and Bastin et al. (1984), among many others. Various generalisations of the least-squares approach have been recently proposed by Kitanidis (1983) in the case of generalized covariances being linear in the parameters.

The variogram identification can also be performed by minimizing a functional of a set of observed interpolation errors. The "mean squared interpolation error" (MSIE) method discussed in this paper and a maximum likelihood method recently described by Bastin and Gevers (1985) lie in this category. The MSIE approach has been previously used by Davis and David

0022-1694/85/$03.30

(1978), Gambolati and Volpi (1979), and Hughes and Lettenmaier (1981) for the calibration of the variogram parameters. An MSIE criterion is also included in the BLUEPACK software (e.g., Delfiner, 1976), in order to compare variogram models [a typical application can be found in Chua and Bras (1982)].

The objective of this paper is to give a fairly systematic presentation of the MSIE method and to illustrate it with two real-life hydrologic applications.

The basic idea which underlies the determination of the identification criterion is that if a variogram model is identified in order to design an optimal interpolator, then it makes sense to use the minimization of the interpolation errors as a criterion for the selection of the best variogram model. The presentation involves a theoretical asymptotic analysis of the MSIE method under the assumption that the parametric variogram model is only an approximation of the true-field variogram: this is certainly a realistic point of view since in most practical applications very simple (often isotropic) models are adopted. A general asymptotic property is demonstrated which does not require any specific assumption on the probability density of the field.

The basic concepts and assumptions are presented in Section 2. The identification method is stated in Sections 3 and 4 together with the theoretical asymptotic analysis aforementioned. Then we describe in some detail the application of the method to the identification of variogram models for a piezometric field (Section 5) and a rainfall field (Section 6).

2. BASIC CONCEPTS AND ASSUMPTIONS

The variogram identification problem is based on four entities:
(a) a random field F;
(b) a set of point-wise scattered observations of a realization of F;
(c) a set of parametric models M; and
(d) a criterion.

Identification, then, is to select that model within the set of models that describes the data best according to these criteria. In this section, we describe entities (a), (b) and (c) in some detail and we state assumptions regarding their properties that will be used later in the paper.

2.1. The random field F and the data

According to the usual definition of random functions (e.g., Papoulis, 1965), F is a family of real valued functions:

$$F = \{z(u, \omega) \mid u \in \mathbb{R}^2, \omega \in \Omega\} \tag{1}$$

where u is a space coordinate, $u = (x, y)$; and ω belongs to an appropriate

probability space Ω. Without loss of generality, we use the notation $z(u)$ to represent the field, omitting the dependence on ω. When u is fixed in $\mathbb{R}^2$, $z(u)$ denotes a random variable. We use the same notation $z(u)$ for a particular realization — this should, however, not lead to any confusion.

Assumption A1: The random field F is intrinsic (Matheron, 1965), i.e.:

(a) the (unknown) mean is stationary:

$$m = \mathrm{E}[z(u)], \qquad u \in \mathbb{R}^2 \tag{2}$$

(b) the (unknown) variogram is stationary:

$$\gamma_F(h) = \tfrac{1}{2}\mathrm{E}[\{z(u)-z(v)\}^2] \qquad \text{with} \qquad h = v-u \tag{3}$$

for any pair (u, v) of points in $\mathbb{R}^2$.

Definition: A generalized increment (GI), $\eta(u_1, u_2, \ldots, u_n)$, is a linear combination of the form:

$$\eta(u_1,u_2,\ldots,u_n) = \sum_{i=1}^{n} \mu_i z(u_i) \qquad \text{with} \qquad \sum_{i=1}^{n} \mu_i = 0 \tag{4}$$

The set $I = \{u_1, u_2, \ldots, u_n\}$ is called the support of η.

Obviously from assumption A1:

$$\mathrm{E}[\eta] = 0 \qquad \text{for any } \eta \tag{5}$$

It is well known that, under assumption A1, a unique "best linear unbiased" interpolate $\hat{z}_F(u_0)$ can be computed from any set $Z_1^N = \{z(u_1), z(u_2), \ldots, z(u_N)\}$:

$$\hat{z}_F(u_0) = \sum_{i=1}^{N} \phi_i z(u_i) \qquad \text{with} \qquad \sum_{i=1}^{N} \phi_i = 1 \tag{6}$$

The coefficients ϕ_i are the solution of the so-called "Kriging system" (Journel and Huijbregts, 1978). The subscript F is used to conceptually distinguish the true interpolate computed with the true (but unknown) variogram, from an approximate interpolate computed with a variogram model, that shall be introduced in Section 2.2. $\hat{z}_F(u_0)$ can be viewed either as a random variable (if Z_1^N is a set of random variables) or as a deterministic number (if Z_1^N is a sample of a field realization). In the latter case we refer to Z_1^N as the *set of data* or the set of observations.

The interpolation error is denoted:

$$e_F(u_0) = z(u_0) - \hat{z}_F(u_0) \tag{7}$$

The following lemma summarizes some well-known properties of $e_F(u_0)$.

Lemma L1:

(a) $e_F(u_0)$ is a GI on the support $I_0 = \{u_0, u_1, \ldots, u_N\}$.

(b) $$\mathrm{E}[e_F^2(u_0)] = -\sum_{i=0}^{N}\sum_{j=0}^{N} \phi_i \phi_j \gamma_F(h_{ij}) \tag{8}$$

with $\phi_0 = -1$ and $h_{ij} = u_j - u_i$.

(c) $\mathrm{E}[e_F(u_0)\,\eta(I_1)] = 0$ for any GI

on the support

$$I_1 = \{u_1, u_2, \ldots, u_N\} = I_0 \backslash \{u_0\} \tag{9}$$

The quantity $\mathrm{E}[e_F^2(u_0)]$ is called the "interpolation error variance" and is denoted $\sigma_F^2(u_0)$.

2.2. The set of models M

In most practical applications, fairly simple isotropic parametric models are used to describe the variograms. Commonly used models are (with $\bar{h} = \|h\|$):

(a) the power-type model,

$$\gamma_M(\bar{h}) = \alpha \bar{h}^\beta, \qquad 0 < \beta < 2 \tag{10a}$$

(b) the logarithmic-type model,

$$\gamma_M(\bar{h}) = \alpha \log(1 + \beta \bar{h}) \tag{10b}$$

(c) the exponential-type model,

$$\gamma_M(\bar{h}) = \alpha[1 - \exp(-\beta \bar{h})] \tag{10c}$$

(d) the Gaussian-type model,

$$\gamma_M(\bar{h}) = \alpha[1 - \exp(-\beta \bar{h}^2)] \tag{10d}$$

(e) the spherical model,

$$\gamma_M(\bar{h}) = \begin{cases} \frac{1}{2}\alpha(3\bar{h}\beta^{-1} - \bar{h}^3\beta^{-3}), & \bar{h} \leqslant \beta \\ \alpha, & \bar{h} \geqslant \beta \end{cases} \tag{10e}$$

When a user chooses one of these expressions for his problem, he actually defines a *set of models*, parameterized by α and β, within which the best model (i.e. the best estimates $\hat{\alpha}$ and $\hat{\beta}$) is to be selected. We denote the set of models by M.

In this paper we restrict ourselves to sets of isotropic models with the general form:

$$\gamma_M(\bar{h}, \alpha, \beta) = \alpha g_M(\bar{h}, \beta) \tag{11}$$

but most of the discussion hereafter can be applied to more complicated parametric models. Note also that all the models (eqs. 10a–e) have the form of eq. 11.

Now, using the Kriging system with the model γ_M instead of the true (unknown) variogram γ_F, one can compute, from Z_1^N, an approximate interpolate $\hat{z}_M$ and an approximate interpolation error variance σ_M^2 for any member of a set of models. Obviously, different interpolates can be obtained for different values of (α, β).

Some basic properties of the approximate interpolates (corresponding to a given set of models) are summarized in the following lemma.

Lemma L2:

(a) The approximate interpolates $\hat{z}_M$ are independent of α and depend only on β:

$$\hat{z}_M(u_0,\beta) = \sum_{i=1}^{N} \lambda_i(\beta) z(u_i), \qquad \sum_{i=1}^{N} \lambda_i(\beta) = 1 \tag{12}$$

(b) The approximate interpolation error variance σ_M^2 is of the form:

$$\sigma_M^2(u_0,\alpha,\beta) = -\alpha \sum_{i=0}^{N}\sum_{j=0}^{N} \lambda_i(\beta)\lambda_j(\beta) g_M(\bar{h}_{ij},\beta), \qquad \lambda_0 = -1 \tag{13}$$

(c) The interpolation error $e_M(u_0,\beta) = z(u_0) - \hat{z}_M(u_0,\beta)$ is a GI on the support $I_0 = \{u_0, u_1, \ldots, u_N\}$

It must be emphasized that σ_M^2 is *not* the variance of e_M but is an estimate of σ_F^2.

3. THE ESTIMATION OF β BY THE MEAN SQUARED INTERPOLATION ERROR (MSIE) METHOD

In this section we consider the problem of estimating β from a finite set of pointwise data $Z_1^N = [z(u_1), \ldots, z(u_N)]$ by the MSIE method. The basic idea is that, if a variogram model is identified in order to design an optimal interpolator, then it makes sense to use the minimization of the interpolation errors as a criterion for the selection of the best model in the model set.

3.1. Description of the method

Having chosen a variogram model $\gamma_M(\bar{h}) = \alpha g_M(\bar{h},\beta)$, we can compute, at each data point u_i, the interpolate $\hat{z}_M(u_i,\beta)$ and the interpolation error $e_M(u_i,\beta)$ based on the other points u_j $(j = 1, \ldots, N; j \neq i)$.

Our guiding principle for the variogram identification is then to select β in such a way that the interpolation errors $e_M(u_i,\beta)$ are as small as possible, in a mean squared sense. Therefore we consider the following criterion:

$$V(\beta) = N^{-1} \sum_{i=1}^{N} e_M^2(u_i,\beta) \tag{14}$$

Then the MSIE estimate of β is defined as the value of β that minimizes $V(\beta)$:

$$\hat{\beta} = \arg\{\min_{\beta} V(\beta)\} \tag{15}$$

3.2. A meaningful asymptotic property of the MSIE *method*

In case of asymptotic convergence of the criterion $V(\beta)$ for large data samples, one can give a very meaningful interpretation of the MSIE method. This interpretation is based on the following theorem:

Theorem: Let:

$$\bar{V}(\beta) = \mathrm{E}[V(\beta)] \tag{16}$$

and

$$\bar{W}(\beta) = N^{-1} \sum_{i=1}^{N} \mathrm{E}[\{\hat{z}_F(u_i) - \hat{z}_M(u_i,\beta)\}^2] \tag{17}$$

Assume that, for large data samples, $V(\beta)$ tends asymptotically to $\bar{V}(\beta)$. Then the minimization of $V(\beta)$ with respect to β is asymptotically equivalent to the minimization of $\bar{W}(\beta)$.

Proof: By assumption, the minimization of $V(\beta)$ is asymptotically equivalent to the minimization of $\bar{V}(\beta)$:

$$\bar{V}(\beta) = N^{-1} \sum_{i=1}^{N} \mathrm{E}[\{z(u_i) - \hat{z}_M(u_i,\beta)\}^2]$$

by eq. 7:

$$\bar{V}(\beta) = N^{-1} \sum_{i=1}^{N} \mathrm{E}[\{\hat{z}_F(u_i) + e_F(u_i) - \hat{z}_M(u_i,\beta)\}^2]$$

$$\bar{V}(\beta) = N^{-1} \sum_{i=1}^{N} \Big\{ \mathrm{E}[\{\hat{z}_F(u_i) - \hat{z}_M(u_i,\beta)\}^2] + 2\mathrm{E}[\{\hat{z}_F(u_i) - \hat{z}_M(u_i,\beta)\} e_F(u_i)] + \sigma_F^2(u_i) \Big\} \tag{18}$$

By lemma L*1*:

$$\mathrm{E}[\{\hat{z}_F(u_i) - \hat{z}_M(u_i,\beta)\} e_F(u_i)] = 0 \tag{19}$$

since $[\hat{z}_F(u_i) - \hat{z}_M(u_i,\beta)]$ is a GI on $\{u_1, \ldots, u_{i-1}, u_{i+1}, \ldots, u_N\}$

therefore

$$\bar{V}(\beta) = \bar{W}(\beta) + N^{-1} \sum_{i=1}^{N} \sigma_F^2(u_i) \tag{20}$$

Obviously $\sigma_F^2(u_i)$ is independent of β.

Then the minimization of $V(\beta)$ is equivalent to the minimization of $\bar{W}(\beta)$ (q.e.d).

Conclusion: It follows from this theorem that, at least asymptotically, the MSIE method selects, in a set of models, the variogram which gives the interpolates $\hat{z}_M(u_i,\beta)$ that are, in a mean square sense, as close as possible to the

optimal interpolates $\hat{z}_F(u_i)$ that could be computed if the true variogram was known. *This conclusion does not require that the true variogram need to be described exactly within the set of models, nor does it require any specific assumption on the probability density of the field.*

Comments

(1) The assumption that $V(\beta)$ converges to $\bar{V}(\beta)$ for large data samples is certainly a reasonable ergodicity assumption for most actual situations. However, the determination of conditions on the field F under which this assumption holds is not a trivial task. This paper is oriented toward applications and we shall not discuss this point further here. A detailed discussion of the convergence of the MSIE method can be found in Bastin (1983).

(2) As we have pointed out, the property just stated does not require that the true variogram can be described by any of the models in the set of models. If such an assumption is imposed, it is evident that the estimate $\hat{\beta}$ converges to the true value of β provided that $V(\beta)$ has a unique minimum. In the applications that we have treated so far, we have always found functionals $V(\beta)$ with a unique minimum as we shall illustrate in the applications.

(3) The MSIE method can be used for random fields with nonstationary polynomial trends just as it has been described. We shall discuss this point in application *1*.

(4) A drawback of the MSIE method is that it does not take into account the geometry of the data points. One would expect that the interpolation error at a point that is fairly distant from most other measuring points would be larger than at a point that lies in a region where the measurements are dense. Yet the criterion gives the same weight to all interpolation errors. One can eliminate this drawback by incorporating the geometry of the measuring points into the criterion using maximum likelihood arguments (Bastin and Gevers, 1985).

4. ESTIMATION OF α USING THE STANDARDIZED MEAN SQUARE ERROR (SMSE) CRITERION

In this section, we consider the problem of estimating α from the interpolation errors $e_M(u_i, \hat{\beta})$.

It follows from lemma L2 that the approximate interpolation error variance $\sigma_M^2(u_i, \alpha, \hat{\beta})$ can be written:

$$\sigma_M^2(u_i, \alpha, \hat{\beta}) = \alpha s_M^2(u, i, \hat{\beta}) \tag{21}$$

where the coefficients $s_M^2(u_i, \hat{\beta})$ can be calculated from $g_M(\bar{h}, \hat{\beta})$.

From lemma L2 it is also clear that we can consider $\sigma_M^2(u_i, \alpha, \hat{\beta})$ as an approximation of the variance of $e_M^2(u_i, \hat{\beta})$. Therefore a straightforward way

for estimating α is to choose an estimate $\hat{\alpha}$ that ensures the consistency between $\sigma_M^2(u_i, \hat{\alpha}, \hat{\beta})$ and $e_M^2(u_i, \hat{\beta})$. A usual criterion to evaluate this consistency (Delfiner, 1976; Gambolati and Volpi, 1979) is the "standardized mean square error" (SMSE):

$$\Sigma(\alpha) = N^{-1} \sum_{i=1}^{N} e_M^2(u_i, \hat{\beta}) / \sigma_M^2(u_i, \alpha, \hat{\beta}) = N^{-1} \sum_{i=1}^{N} e_M^2(u_i, \hat{\beta}) / \alpha s_M^2(u_i, \hat{\beta}) \qquad (22)$$

Then the estimate $\hat{\alpha}$ can be defined by $\Sigma(\hat{\alpha}) = 1$, i.e.:

$$\hat{\alpha} = N^{-1} \sum_{i=1}^{N} e_M^2(u_i, \hat{\beta}) / s_M^2(u_i, \hat{\beta}) \qquad (23)$$

It must be noticed that a maximum likelihood interpretation of this expression of $\hat{\alpha}$ can also be derived (Bastin and Gevers, 1985).

5. APPLICATION TO A PIEZOMETRIC FIELD

5.1. Motivation of the variogram identification

A typical application of the BLU interpolation in random fields is the optimal contour mapping of piezometric levels (i.e. water-table levels) in a groundwater reservoir. Such a contour mapping requires the estimation of the piezometric level at all nodes of a meshed network covering the domain (in order to establish a chart of the piezometry) from measurements taken in a few wells scattered within the reservoir. Such a piezometric chart has been used as an input of an identification procedure whose objective was the modelling of groundwater flow in an aquifer of the Dyle river basin in Belgium (Bastin, 1981; Bastin and Duqué, 1981).

5.2. Description of the data

The piezometric level has been observed in 28 wells during October and November 1977: the data-point coordinates and the measured piezometric levels are indicated in Table I. An experimental variogram computed from these data is shown in Fig. 1: it is drawn using 16 distance intervals, each of 276-m length.

5.3. Identification of a variogram model by the MSIE *method*

From the data of Table I, the parameters α and β of various variogram parametric models were estimated, under assumption A*1*, with the methods described in the previous sections. The results are shown in Table II and lead to the following comments:

TABLE I

x-, y-coordinates and observed waterlevels z for 28 piezometers

No.	x (m)	y (m)	z (m)	No.	x (m)	y (m)	z (m)
1	165,390	153,810	56.00	*15*	168,042	150,499	110.71
2	168,860	153,365	89.47	*16*	167,965	150,384	110.00
3	169,040	149,456	116.60	*17*	167,115	149,340	103.66
4	167,470	152,785	84.73	*18*	167,013	149,312	104.03
5	166,650	152,000	83.00	*19*	166,325	149,100	98.07
6	167,610	152,175	89.08	*20*	165,575	148,600	85.50
7	167,608	151,651	90.00	*21*	164,500	149,625	60.32
8	166,057	151,156	83.12	*22*	168,971	151,892	97.28
9	166,329	150,786	86.93	*23*	168,871	150,874	113.80
10	166,477	150,590	88.48	*24*	165,350	151,625	60.00
11	167,345	151,040	91.20	*25*	165,850	151,650	70.00
12	167,899	150,891	107.04	*26*	165,650	149,325	80.00
13	167,629	150,603	105.80	*27*	165,500	149,675	70.00
14	167,972	150,942	109.17	*28*	165,875	150,203	80.00

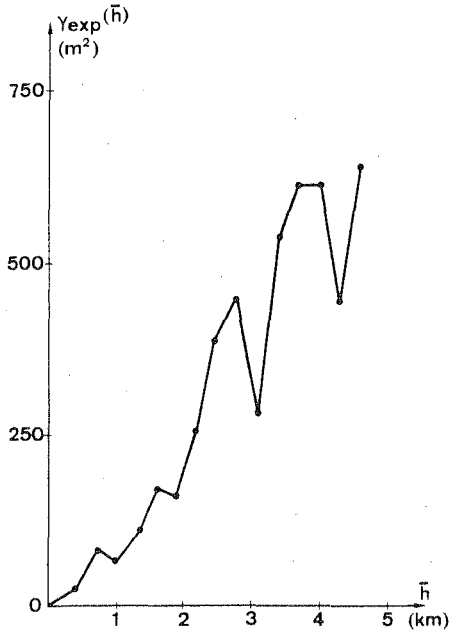

Fig. 1. Experimental variogram.

TABLE II

MSIE identification results for various parametric variogram models

Variogram model	$\hat{\alpha}$	$\hat{\beta}$	$V(\hat{\beta})$	$Q=\sqrt{V(\hat{\beta})}$
$\gamma(\bar{h})=\alpha\bar{h}^{\beta}$	30.82	1.44	9.45	3.07
$\gamma(\bar{h})=\alpha[1-\exp(-\beta\bar{h}^2)]$	155.9	0.99	28.52	5.04
$\gamma(\bar{h})=\alpha\log(1+\beta\bar{h})$		$\to 0$		
$\gamma(\bar{h})=\alpha[1-\exp(-\beta\bar{h})]$		$\to 0$		

(a) As can be expected from the shape of the experimental variogram, only models with positive curvature (i.e. the power- and the Gaussian-type models) can be reasonably estimated. Indeed, the method converges to a meaningless estimate $\hat{\beta}=0$ for the models with negative curvature.

(b) The best model selected by the MSIE method is the following power-type model:

$$\gamma(\bar{h}) = 30.82\bar{h}^{1.44} \tag{24}$$

with a water-level mean square error $Q = 3.07$ m (while $Q = 5.34$ m with the best Gaussian-type model).

(c) The criterion $V(\beta)$ for the power-type model is shown in Fig. 2: it has a unique well-pronounced minimum value.

In Table III, we give the estimates $\hat{\alpha}_{LS}$ and $\hat{\beta}_{LS}$ obtained from a least-squares (LS) fitting of the parametric models on the experimental variogram [the details on this least-squares estimation are described in Bastin and Gevers (1985)]. The mean square error $Q=\sqrt{V(\hat{\beta}_{LS})}$ and the SMSE $\Sigma(\hat{\alpha}_{LS})$ are also indicated. Fig. 3 illustrates graphically the identified models.

We see that, for the power-type models, the mean square errors Q obtained with the MSIE method and the LS methods are quite close (3.07 and 3.27, respec.). Nevertheless, these models are not equivalent since the values of $\hat{\alpha}$ (and, therefore, also the interpolation error variance σ_M^2) are very different (30.82 and 91.49, respec.). Furthermore, the SMSE $\Sigma(\hat{\alpha}_{LS})$ are not admissible (0.26 and 0.56, respectively, instead of 1 as expected from a good variogram model, see Section 4). Therefore, we believe that the LS models must be rejected in spite of a very good fit to the experimental variogram. This is an enlightening illustration of the fact that the variogram model

> "cannot rely entirely upon the experimental variogram"

(Gambolati and Volpi, 1979) and of the

> "obvious lack of robustness of the least squares variogram identification in case of scarce data"

as it resorts from simulations of Bastin and Gevers (1985).

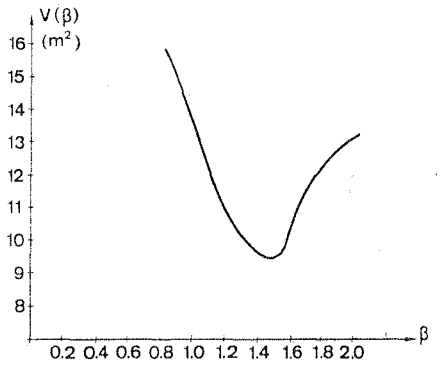

Fig. 2. Criterion $V(\beta)$ for a power-type model.

TABLE III

Least-squares fitting of parametric models to the experimental variogram

Variogram model	$\hat{\alpha}_{LS}$	$\hat{\beta}_{LS}$	$Q = \sqrt{V(\hat{\beta}_{LS})}$	$\Sigma(\hat{\alpha}_{LS})$
$\gamma(\bar{h}) = \alpha \bar{h}^{\beta}$	91.48	1.29	3.27	0.26
$\gamma(\bar{h}) = \alpha[1 - \exp(-\beta \bar{h}^2)]$	729	0.08	13.82	0.56

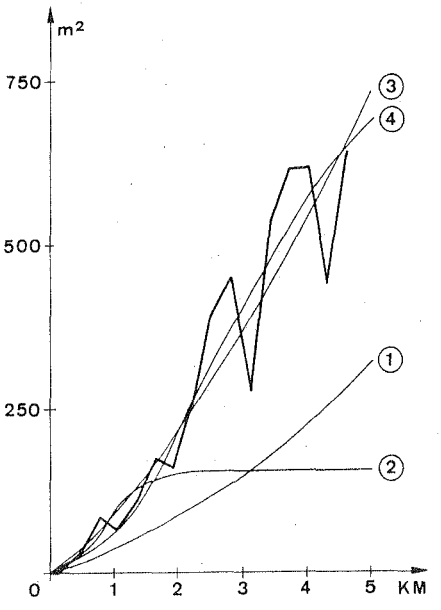

Fig. 3. Estimated variogram models (*1* = power-type model — MSIE; *2* = Gaussian-type model — MSIE; *3* = power-type model — LS; *4* = Gaussian-type model — LS).

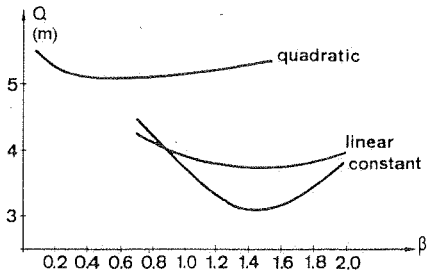

Fig. 4. Criterion $Q = \sqrt{V(\hat{\beta})}$ for different trends.

TABLE IV

MSIE identification results, with a power-type model, for various polynomial trends

Trend, structure	$\hat{\beta}$	Q
Constant	1.44	3.07
Linear	1.38	3.76
Quadratic	0.45	5.11

5.4. Non-stationary polynomial trends

The MSIE identification method can also be used to identify variogram models of fields with a non-stationary mean (or "trend") and a stationary variogram. The most commonly used trend structures are polynomials; here we restrict ourselves to linear and quadratic polynomials of the form:

$$\text{(linear)} \quad \mathrm{E}[z(u)] = a_0 + a_1 x + a_2 y \tag{25}$$

$$\text{(quadratic)} \quad \mathrm{E}[z(u)] = a_0 + a_1 x + a_2 y + a_3 x^2 + a_4 y^2 + a_5 xy \tag{26}$$

It is well known that BLU interpolation can be constrained by such trends even if the coefficients a_i are unknown. Then constrained interpolation errors $e_M(u_i, \beta)$ and a constrained criterion $V(\beta)$ can also be computed and compared with the results of Section 5.3. In case of power-type models, the comparison illustrated in Fig. 4 and Table IV, shows that the MSIE Q increases with the polynomial trend orders.

6. APPLICATION TO RAINFALL FIELDS

6.1. Motivation of the variogram identification

The flash floods in the Cevennes Mountains (southeast of France) which are sometimes catastrophic (1933, 1958, 1976, 1980), have led the public

authorities of the Gard Province to implement a real-time flood forecasting system (Obled and Creutin, 1982). The main purpose of this system is the flood forecasting on small watersheds (300—1000 km^2) with short response times (a few hours).

Both unit-hydrograph and ARMAX single-input—single-output flood forecasting models have been developed (Versiani, 1983). The input of these models is a linear estimate of the hourly mean areal rainfall denoted:

$$P^*(k) = \sum_{i=1}^{N} \lambda_{ik} z_i(k) \tag{27}$$

where k is a discrete time index (time step = 1 hr.) and $z_i(k)$ is the hourly rainfall depth at the ith raingauge.

Several well-known methods have been used for the determination of the weighting coefficients λ_{ik}: e.g., Thiessen method, spline functions, Kriging (Lebel and Creutin, 1983). Irrespective of the method of computation of the λ_{ik}, the variance of $P^*(k)$ can be written:

$$\sigma_P^2(k) = 2A^{-1} \sum_{i=1}^{N} \lambda_{ik} \int_A \gamma_F(u - v_i, k)\, dv - \sum_{i=1}^{N} \sum_{j=1}^{N} \lambda_{ik} \lambda_{jk} \gamma_F(v_j - u_i, k)$$

$$+ A^{-2} \int_A \int_A \gamma_F(v - u, k)\, dv du \tag{28}$$

if, *for a fixed* k, the hourly rainfall depths $z_i(k)(i = 1, \ldots, N)$ are viewed as pointwise realizations of a random field with variogram (see eq. 3):

$$\gamma_F(h, k) = \gamma_F(v - u, k)$$

In expression (28), A denotes the watershed surface.

It follows from this expression that the calculation of $\sigma_P^2(k)$ needs a preliminary identification of a variogram model. Another motivation is that the knowledge of the variogram of rainfall fields allows for the computation of mean areal GRADEX's which are known to be efficient tools for the determination of extreme flood values (Lebel and Guillot, 1983; Lebel, 1984).

6.2. Description of the data

We have analyzed all the large rainfall events on the Cevennes during the last ten years. We have restricted ourselves to the fall season since it is the season of the major flash floods. We present the variogram identification results that we have obtained on the Gardon d'Anduze river basin, using a network of 34 recording raingauges which are shown in Fig. 5 and Table V. The 103 strongest hourly rainfalls have been selected and distributed in two samples according to two types of spatial structure: sample A involves 49 events with a strong cell centered over the basin while sample B involves 54 events with a more complex structure. An illustration is given in Fig. 6 and

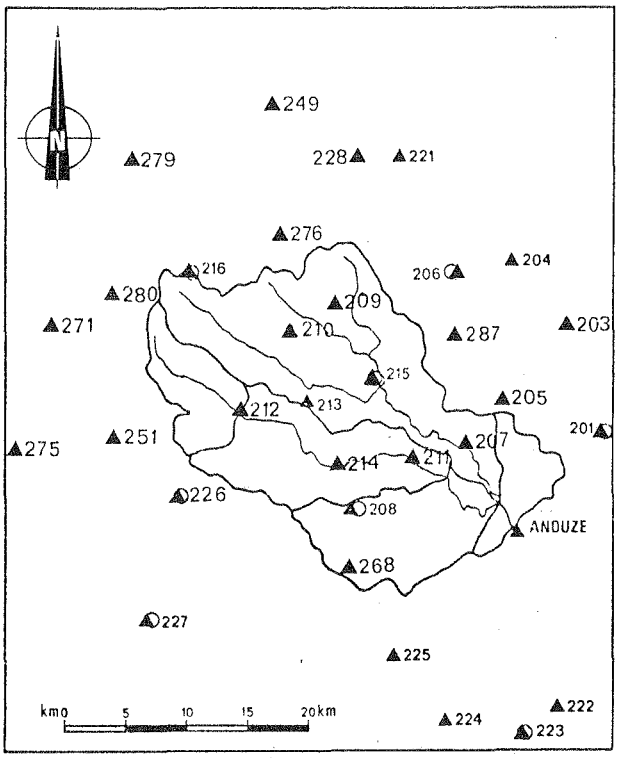

Fig. 5. Gardon d'Anduze watershed and raingauge network (▲ = station).

Table VI summarizes some statistical characteristics of the data, namely the spatial sample mean and the spatial sample variance of each event, defined as follows:

$$\bar{P}(k) = N^{-1} \sum_{i=1}^{N} z_i(k) \tag{29}$$

$$S^2(k) = N^{-1} \sum_{i=1}^{N} [z_i(k) - \bar{P}(k)]^2 \tag{30}$$

6.3. Basic assumption

Following a climatological approach for the identification of rainfall fields variograms described by Bastin et al. (1984), we adopt a parametric structure of the form:

$$\gamma_M(\bar{h}, k) = \alpha(k) g_M(\bar{h}, \beta) \tag{31}$$

With this structure all the time nonstationarity (i.e. the dependence on the

TABLE V

Coordinates (km) and names of the raingauges

No.	x	y	
212	66.5	64.8	St. André de Valborg
202	89.2	55.0	Anduze
203	93.3	71.5	La Grand Combe
204	88.9	76.8	Ste. Cécile
205	88.0	65.5	St. Paul la Costé
206	83.8	76.0	Collet de Dézé
207	85.1	61.8	Mialet
208	75.7	56.9	Soudorgues
209	74.3	73.4	St. Germain de Calbé
210	70.5	71.1	Fabregues
211	80.6	60.8	St. Jean Du Gard
201	97.0	63.0	Alès
213	71.8	65.5	St. Roman de Tousque
214	74.4	60.3	St. Martin de Corçon
215	77.5	67.5	St Étienne
216	62.5	76.0	Barre des Cevennes
221	79.4	85.3	Soleyrol
222	92.5	40.8	Barrage de Rouvière
223	90.0	38.7	Quissac
224	83.2	39.7	Barrage de Ceyrac
225	79.0	45.0	St. Hippolyte du For
226	61.5	58.0	Valleraugue
227	59.0	48.0	Le Vigan
228	76.0	85.2	St. Hippolyte du For
249	69.0	89.5	Pont de Montvert
251	56.1	62.6	Mont Aigoual
263	80.2	26.6	Valflaunes
268	75.5	52.0	Colognac
275	47.9	61.6	Camprieu
276	69.6	78.9	Cassgnas
279	57.6	85.0	Florac
280	55.9	74.2	Les Vanels
287	84.0	70.8	Mas Villard
271	51.0	71.8	Perjuret

time index k) is concentrated in the scale factor $\alpha(k)$ (which has to be estimated separately for each event), while the factor $g_M(\bar{h}, \beta)$ is time invariant and can be estimated once and for all from the complete set of data.

It must be emphasized that, in case of a bounded variogram model, this approach is completely equivalent to L.S. Gandin's climatological approach (Gandin, 1965; see also Creutin and Obled, 1982).

Consider that the first-order spatial increments of each event have been standardized as follows:

$$[z_i(k) - z_j(k)]/\mathrm{S}(k) \tag{32}$$

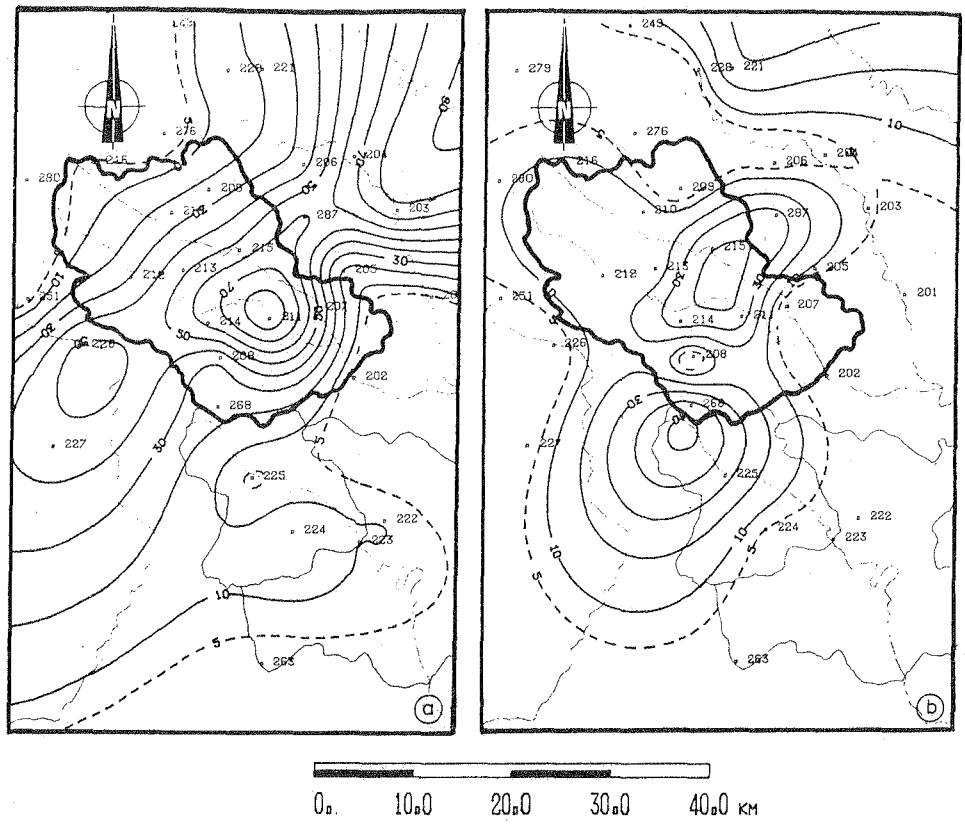

Fig. 6. a. Strong hourly rainfall centered over the basin.
b. More complex structure with a cell on the border of the basin.

TABLE VI

Spatial sample mean and sample standard deviation of the hourly rainfalls in each sample

Sample A			Sample B		
date (year/month/ day/hour)	mean $\bar{P}(k)$	S.D. $S(k)$	date (year/month/ day/hour)	mean $\bar{P}(k)$	S.D. $S(k)$
75/09/30/08	72.9	94.6	73/11/05/01	25.0	30.8
75/09/30/10	67.1	88.6	73/11/05/03	13.6	23.3
75/09/30/12	165.8	191.5	73/11/05/05	35.9	46.0
75/09/30/13	163.9	162.2	73/11/05/07	52.3	73.9
75/09/30/14	121.2	138.7	73/11/05/09	32.7	43.5
76/08/29/01	85.3	85.3	73/11/05/11	47.3	53.7
76/08/29/02	109.1	125.0	73/11/05/13	40.9	52.3
76/08/29/03	93.6	85.5	74/09/16/20	168.2	244.9
76/08/29/05	66.3	86.6	74/09/16/22	63.6	99.2
76/08/29/06	68.6	100.3	74/09/16/24	103.6	130.5

TABLE VI (*continued*)

Sample A			Sample B		
date (year/month/ day/hour)	mean $\bar{P}(k)$	S.D. $S(k)$	date (year/month/ day/hour)	mean $\bar{P}(k)$	S.D $S(k)$
76/09/12/05	62.2	86.0	74/09/17/02	108.2	135.7
76/09/12/06	227.3	282.8	74/09/17/03	159.5	207.1
76/09/12/07	262.5	247.6	74/09/17/06	142.3	183.8
76/09/12/08	181.0	178.0	76/08/28/14	77.3	104.8
76/09/12/09	188.5	179.8	76/08/28/15	66.2	120.5
76/09/12/10	137.7	183.0	76/09/12/20	43.1	48.3
76/11/09/16	81.6	72.9	76/09/12/21	110.8	82.7
76/11/09/18	55.7	48.4	76/09/12/22	63.8	58.9
76/11/09/20	71.2	46.5	79/10/24/18	33.5	31.6
76/11/09/22	79.2	50.1	79/10/24/20	33.5	23.9
76/11/09/24	83.9	50.2	79/10/24/23	46.9	18.5
76/11/10/02	90.0	60.5	79/10/25/01	57.3	20.5
76/11/10/03	101.9	71.1	79/10/25/04	42.3	32.6
76/11/10/06	81.6	62.4	79/10/25/06	62.7	32.0
77/10/23/07	93.6	112.1	79/10/25/10	68.5	31.0
77/10/23/11	108.2	106.6	79/10/25/12	56.9	16.5
77/10/23/12	131.0	165.1	79/10/25/16	46.5	24.4
77/10/23/13	139.0	146.3	79/10/25/20	40.8	20.7
77/10/23/14	106.0	132.1	79/10/25/22	50.4	16.8
77/10/23/16	73.9	64.5	79/10/25/24	55.0	29.6
79/10/04/20	104.2	135.9	79/10/26/02	36.2	31.6
79/10/04/21	165.7	201.0	79/10/26/03	53.8	41.8
79/10/04/22	62.9	79.6	79/10/26/05	72.7	35.8
79/10/04/23	30.8	100.9	79/10/26/08	39.9	18.2
79/10/04/24	39.0	52.8	79/10/26/10	59.2	28.1
79/10/07/01	47.2	30.2	79/10/26/12	48.5	33.5
70/10/07/03	56.0	51.9	79/10/26/14	54.6	45.0
79/10/07/05	57.9	45.6	79/10/26/16	50.0	27.7
79/10/07/07	46.6	30.9	79/10/26/18	58.5	40.4
79/10/07/10	47.7	31.2	79/10/26/19	53.1	23.5
79/10/07/12	54.1	43.9	79/10/26/22	33.0	15.4
79/10/07/15	69.6	63.4	80/09/20/18	23.7	34.9
80/08/15/11	55.8	56.9	80/09/20/20	71.2	108.7
80/08/15/12	126.4	125.9	80/09/20/23	9.6	13.3
80/08/15/15	70.4	81.6	80/09/20/24	32.5	48.9
80/10/16/14	55.7	57.3	80/09/21/02	38.3	38.5
80/10/16/16	87.0	104.0	80/09/21/04	31.7	55.8
80/10/16/18	64.3	65.5	80/09/21/05	35.0	85.4
80/10/16/20	152.6	128.2	80/09/21/06	25.4	59.5
			80/09/21/08	40.4	78.5
			80/09/21/09	39.2	72.6
			80/09/21/11	37.9	90.9
			80/09/21/12	21.2	43.5
			80/09/21/14	17.5	31.9

S.D. = standard deviation.

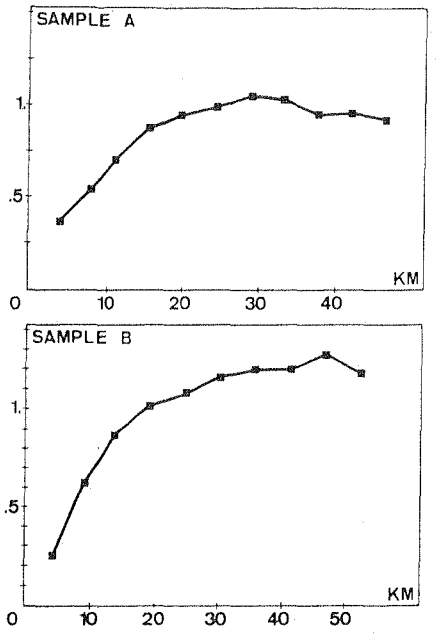

Fig. 7. Climatological experimental variograms.

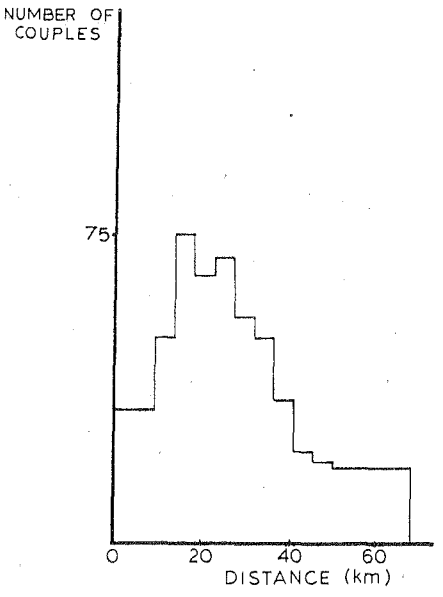

Fig. 8. Distribution of the data-point couples with respect to the distance intervals.

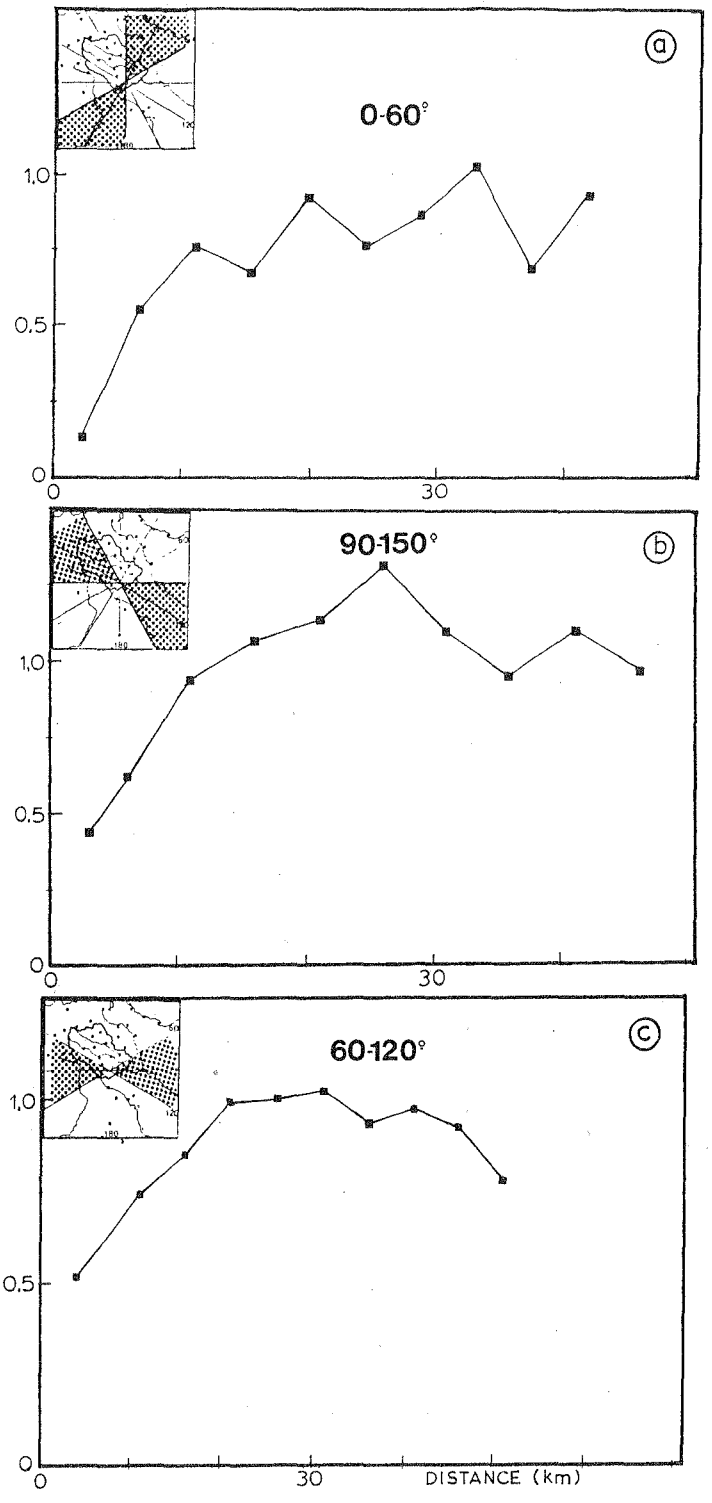

Fig. 9. Climatological experimental variograms for three directions.

Then the basic assumption that underlies the choice of the variogram structure eq. 31 is that all the standardized observations in a given sample (A or B) are realizations of a unique random field with variogram model $g_M(\bar{h}, \beta)$ (which we call the climatological variogram). Such an assumption is certainly reasonable within the context of our application (see Section 6.1), since the data samples involve homogeneous data. Furthermore, it is absolutely needed for real-time forecasting purpose (with 1-hr. time step): the automatic fitting of a variogram model for each event would be too much time consuming.

6.4. The experimental climatological variograms

The experimental climatological variogram has been drawn for each data sample, with the standardization (32). They are presented in Fig. 7.

A division into 15 distance intervals has been adopted. However, intervals *1*, *2* and *12—15* have been aggregated. The distribution of the data-point couples with respect to the distance intervals is shown in Fig. 8.

As can be expected from the standardization (32), the sill of the experimental variograms is nearly one. The search for preferred directions did not give significant results as can be seen in Fig. 9.

6.5. Climatological variogram identification by the MSIE *method*

In view of the shape of the experimental variograms, a spherical and a power-type structure are tried:

spherical model:

$$g_M(\bar{h}, \beta) = \begin{cases} \frac{1}{2}(3\bar{h}\beta^{-1} - \bar{h}^3\beta^{-3}), & 0 \leqslant \bar{h} \leqslant \beta \\ 1, & \bar{h} \geqslant \beta \end{cases} \tag{33}$$

power-type model:

$$g_M(\bar{h}, \beta) = \bar{h}^{\beta} \tag{34}$$

For each model and for each event we can compute the MSIE:

$$V_k(\beta) = N^{-1} \sum_{i=1}^{N} e_M^2(u_i, \beta, k) \tag{35}$$

Then, a global MSIE criterion over all the events is defined as:

$$V(\beta) = K^{-1} \sum_{k=1}^{K} V_k(\beta) \tag{36}$$

with K the number of events in a sample ($K = 49$ and $= 54$ for samples A and B, respectively).

TABLE VII

Values of the criterion $V(\beta)$

Sample A

Spherical:									
β = range (km)	1	10	15	20	25	30	35	40	50
$V(\beta)$ (mm^2)	170.3	123.5	109.1	99.0	91.4	92.9	99.1	105.5	126.2
Power type:									
β	0.1	0.3	0.5	0.6	0.7	0.8	0.9	1.0	1.5
$V(\beta)$ (mm^2)	159.8	112.6	96.8	94.2	93.5	98.6	105.0	114.4	146.5

Sample B

Spherical:									
β = range (km)	1	10	15	20	25	30	35	40	50
$V(\beta)$ (mm^2)	118.8	102.5	92.8	75.4	71.2	74.6	81.2	88.5	97.3
Power type:									
β	0.1	0.3	0.5	0.6	0.7	0.8	0.9	1.0	1.5
$V(\beta)$ (mm^2)	130.0	105.1	92.1	81.8	80.4	89.5	101.3	101.6	138.9

TABLE VIII

Values of $V(\beta)$ with 12 stations inside the watershed

Spherical:									
β = range (km)	1	10	15	20	25	30	35	40	50
$V_{12}(\beta)$ (mm^2)	180.1	130.1	114.2	98.2	90.3	92.8	98.6	105.1	120.0
Power type:									
β	0.1	0.3	0.5	0.6	0.7	0.8	0.9	1.0	1.5
$V_{12}(\beta)$ (mm^2)	166.3	112.5	96.2	92.8	90.5	96.7	104.1	111.0	140.2

The minimization of $V(\beta)$, in each sample and for each model, gives the results presented in Table VII. They lead to the following comments:

(1) As can be expected from the shape of the experimental variogram, the spherical model (with a sill) is better than the power-type model.

(2) With a spherical model, we obtain the same optimal value of $\hat{\beta} \simeq 25$ km (i.e. the same "range") for both samples A and B. This is an important *cross-validation* result since the samples are independent and involve rainfall events with very different spatial structure.

(3) The MSIE $V(\hat{\beta})$ is larger for sample A than for sample B: the reason is that the rainfall events in sample A are heavier, as can be seen from Table VI.

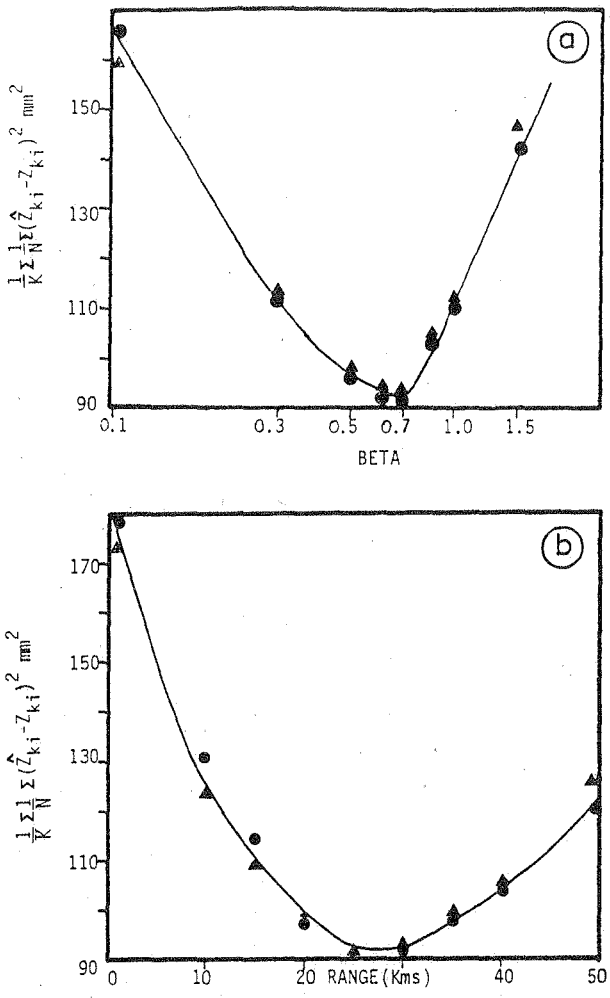

Fig. 10. Criterion $V(\beta)$ for sample A, with the power-type (a) and the spherical model (b) (• = with 12 raingauges; ▲ = with 34 raingauges).

(4) If we restrict the computation of each $V_k(\beta)$ to the twelve stations located inside the watershed (but computing the interpolation errors e_M from the 34 available stations), then we obtain the results of Table VIII, which are very similar to the results with 34 stations as is clearly shown in Fig. 10.

6.6. Nugget effect

The question of whether or not there is a nugget effect is difficult to solve from the examination of the experimental variogram when few data points are near one another. In this case, indeed, the extrapolation of the

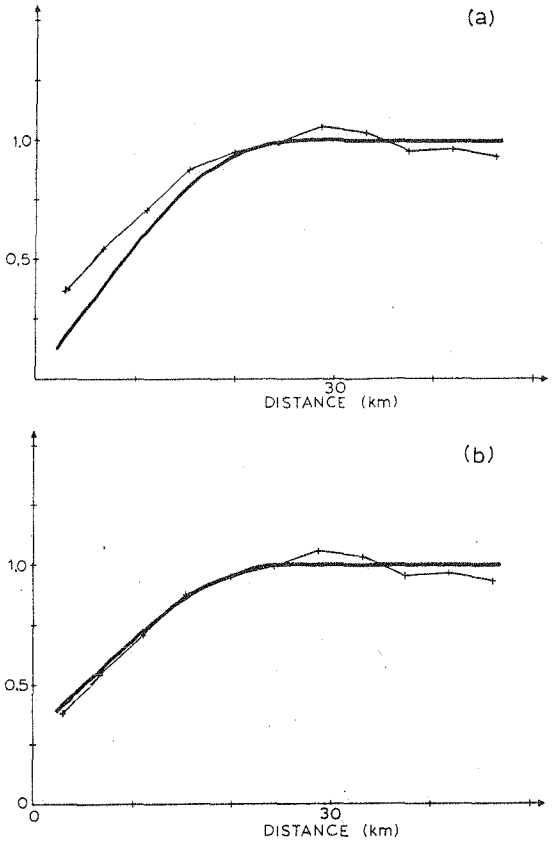

Fig. 11. Spherical model: (a) MSIE; and (b) manual fitting.

TABLE IX

Criterion $V(\beta)$ with respect to the nugget effect

Nugget	0	0.05	0.10	0.15	0.20	0.30	0.40	0.50	1.00
$\beta = 25$	91.4	91.0	91.9	92.7	95.0	112.3	120.7	128.2	171.5
$\beta = 30$	92.9	91.8	92.1	92.9	95.3	112.4	120.9	128.0	171.5

experimental variogram toward the origin is hazardous: this is certainly one of the main drawbacks of manual or LS fitting of parametric models to experimental variograms. From this point of view, the MSIE method can be more reliable.

We show, in Fig. 11, the spherical model that has been estimated above ($\beta = 25$ km) and a spherical model that could be reasonably fitted manually to the experimental variogram. The main difference is the nugget effect which appears to be nonnegligible in the manually fitted model.

TABLE X

Estimates $\hat{\alpha}_0$

Sample	$\hat{\alpha}_0$
A	1.03
B	1.12

In order to study this issue, we have computed the MSIE's for different values of β and of the nugget. The results are given in Table IX: they show that a non-zero nugget does not improve in any way the interpolation performance.

6.7. Estimation of α

In view of the results of the previous sections, we opt for a spherical variogram of the form ($\bar{h}$ in km):

$$\gamma(\bar{h},k) = \begin{cases} \alpha(k)\,[1.5(\bar{h}/25) - 0.5\,(\bar{h}/25)^3\,], & 0 \leqslant \bar{h} \leqslant 25 \\ \alpha(k), & \bar{h} \geqslant 25 \end{cases} \tag{37}$$

Clearly the time-varying parameter $\alpha(k)$ is closely related to the sample variance $S^2(k)$ since, ideally, one should have $\alpha(k) = S^2(k)$ if the variogram model was the true-field variogram and if the sample variance was the true-field variance. Therefore, we adopt the following expression:

$$\alpha(k) = \alpha_0 S^2(k) \tag{38}$$

The values of $S^2(k)$ are known and given in Table VI.

The unknown parameter α_0 can then be estimated using the following version of the SMSE criterion:

$$\hat{\alpha}_0 = (NK)^{-1} \sum_{k=1}^{N} \sum_{i=1}^{N} e_M^2(u_i,\hat{\beta},k)/S^2(k)s_M^2(u_i,\hat{\beta},k) \tag{39}$$

The results, given in Table X, show that $\hat{\alpha}_0$ is close to one for both samples as can be expected. For events of sample A (with a rainfall cell centered over the basin), we see that the sample variance $S^2(k)$ can be taken as the estimate of $\alpha(k)$. For the more complex events of sample B, the sample variance $S^2(k)$ has to be slightly enlarged ($\hat{\alpha}_0 = 1.12$), probably due to a lesser homogeneity of the sample. For reason of safety, we have suggested to the users the value $\hat{\alpha}_0 = 1.12$ for all the future events.

We could also estimate $\alpha(k)$ by using the SMSE criterion separately for each event: however, this would be too much computation time consuming for real-time operation since it requires, at each time step, the numerical

resolution of $(N-1)$ large linear systems in order to calculate the interpolation errors e_M.

The solution we have adopted is very simple: only the calculation of the sample variance $S^2(k)$ is required, every hour. Then the variogram model of the hourly rainfall of interest is completely specified and ready for use by the flood forecasting routine.

7. CONCLUSION

We have given a systematic presentation of the MSIE variogram identification method. The basic idea of this presentation is that of disconnecting the variogram model assumptions from the probabilistic structure of the "true" field. This is certainly a realistic point of view since in most applications very simple (often isotropic) models are adopted and we are never sure that the true field can be exactly described by one of these models. With this point of view, a general asymptotic result is demonstrated which leads to a very meaningful interpretation of the MSIE method. Furthermore consistency of the $\hat{\beta}$ estimate is an immediate consequence of this result.

Then we have illustrated the MSIE method with two hydrologic applications:

(1) In the piezometric field application, the variogram model is a basic tool for the contour mapping of the water level. From the results we conclude that:

(a) the MSIE criterion is an efficient tool to discriminate between alternative variogram models; and

(b) in case of scarce data (here 28 pointwise observations) the models obtained with the MSIE method can differ substantially from those derived from the experimental variogram: a theoretical analysis of the robustness of the various identification methods with small data sets would be very useful.

(2) In the rainfall field application, the variogram model is needed to calculate mean areal rainfall variances and mean areal GRADEX. A global climatological variogram is identified: in the present case a very large data set is available (3502 pointwise observations) and the best model turns out to be very close to the experimental variogram. Furthermore an interesting cross-validation result is that the parameter estimates obtained from two subsamples of the complete data set are very close.

ACKNOWLEDGMENT

The authors are thankful to Professors C. Obled (Grenoble) and M. Gevers (Louvain) for helpful discussions and suggestions.

REFERENCES

Bastin, G., 1981. Identification of steady-state distributed systems with space-variable parameters. Proc. 8th I.F.A.C. (Int. Fed. Autom. Control) World Congr., Kyoto, 2: 64—69.

Bastin, G., 1983. A theoretical analysis of some variogram identification methods. Louvain Univ., Louvain, Lab. Autom. Anal. Systèmes, Inter. Rep. (unpublished).

Bastin, G. and Duqué, C., 1981. Modelling of steady-state groundwater flow systems: deterministic and stochastic approaches. Proc. IASTED (Int. Assoc. Sci. Technol. Dev.) Symp. on Modelling, Identification and Control, Davos, pp. 10—16.

Bastin, G. and Gevers, M., 1985. Identification and optimal estimation of random fields from scattered pointwise data. Automatica, 21(2) (in press).

Bastin, G., Lorent, B., Duqué, C. and Gevers, M., 1984. Optimal estimation of the average areal rainfall and optimal selection of the rain gauge locations. Water Resour. Res., 20(4): 463—470.

Chua, S.H. and Bras, R.L., 1982. Optimal estimates of mean areal precipitation in regions of orographic influence. J. Hydrol., 57: 23—48.

Creutin, J.D. and Obled, C., 1982. Objective analyses and mapping techniques for rainfall fields: an objective comparison. Water Resour. Res., 18(2): 413—431.

David, M., 1977. Geostatistical Ore Reserve Estimation. Elsevier, Amsterdam.

Davis, M.W.D. and David, M., 1978. Automatic kriging and contouring in the presence of trends. J. Can. Pet. Technol., 17: 90—99.

Delfiner, P., 1976. Linear estimation of nonstationary spatial phenomena. In: M. Guarascio, M. David and C. Huijbregts (Editors), Advanced Geostatistics in the Mining Industry. D. Reidel, Dordrecht, pp. 49—68.

Delfiner, P. and Delhomme, J.P., 1975. Optimum interpolation by kriging. In: J.C. Davis and M.J. McCullogh (Editors), Display and Analysis of Spatial Data. Wiley, New York, N.Y., pp. 96—114.

Gambolati, G. and Volpi, G., 1979. Groundwater contour mapping in Venice by stochastic interpolators. Water Resour. Res., 15(2): 281—290.

Gandin, L.S., 1965. Objective Analysis of Meteorological Fields. Israel Program for Scientific Translations, Jerusalem.

Hughes, J.P. and Lettenmaier, D.P., 1981. Data requirements for kriging: estimation and network design. Water Resour. Res. 17(6): 1641—1650.

Journel, A.G. and Huijbregts, Ch.J., 1978. Mining Geostatistics. Academic Press, New York, N.Y.

Kitanidis, P.K., 1983. Statistical estimation of polynomial generalized covariance functions and hydrologic applications. Water Resour. Res., 19(4): 909—921.

Lebel, T., 1984. Moyenne spatiale de la pluie sur un bassin versant: estimation optimale, génération stochastique et GRADEX des valeurs extrêmes. Thèse de Docteur-Ingénieur, Institut National Polytechnique de Grenoble, Grenoble.

Lebel, T. and Creutin, J.D., 1983. Areal rainfall estimation, forecast and simulation over small watersheds subject to major flash floods. 5th A.M.S. (Am. Meteorol. Soc.) Conf. on Hydrometeorology, Tulsa, Okla.

Lebel, T. and Guillot, P., 1983. Statistical analysis of point and areal hourly rainfalls: application to design flood by the GRADEX method. 5th A.M.S. (Am. Meteorol. Soc.) Conf. on Hydrometeorology, Tulsa, Okla.

Matheron, G., 1965. Les variables régionalisées et leur estimation. Masson, Paris.

Obled, C. and Creutin, J.D., 1982. Rainfall related problems in operating the Gard flood warning system. Proc. A.W.R.A. (Am. Water Res. Assoc.) Int. Symp. on Hydrometeorology, Denver, Colo., pp. 159—169.

Papoulis, A., 1965. Probability, Random Variables and Stochastic Processes. McGraw-Hill, New York, N.Y.

Versiani, B., 1983. Modélisation de la relation pluie—débit pour la prévision des crues. Thèse de Docteur-Ingénieur, Institut National Polytechnique de Grenoble, Grenoble.